PHILOSOPHICAL TRANSACTIONS A

royalsocietypublishing.org/journal/rsta

Research

Cite this article: Wittemer M, Schröder J-P, Hakelberg F, Kiefer P, Fey C, Schuetzhold R, Warring U, Schaetz T. 2020 Trapped-ion toolkit for studies of quantum harmonic oscillators under extreme conditions. *Phil. Trans. R. Soc. A* **378**: 20190230.
http://dx.doi.org/10.1098/rsta.2019.0230

Accepted: 25 March 2020

One contribution of 12 to a discussion meeting issue 'The next generation of analogue gravity experiments'.

Subject Areas:
atomic and molecular physics, quantum physics, cosmology

Keywords:
quantum simulation, trapped atomic ion, non-adiabatic control, squeezing

Author for correspondence:
Matthias Wittemer
e-mail:
matthias.wittemer@physik.uni-freiburg.de

Electronic supplementary material is available online at https://doi.org/10.6084/m9.figshare.c.5011307.

Trapped-ion toolkit for studies of quantum harmonic oscillators under extreme conditions

Matthias Wittemer[1], Jan-Philipp Schröder[1], Frederick Hakelberg[1], Philip Kiefer[1], Christian Fey[2], Ralf Schuetzhold[3,4], Ulrich Warring[1] and Tobias Schaetz[1]

[1]Albert-Ludwigs-Universität Freiburg, Physikalisches Institut, Hermann-Herder-Strasse 3, 79104 Freiburg, Germany
[2]Zentrum für Optische Quantentechnologien, Universität Hamburg, Fachbereich Physik, Luruper Chaussee 149, 22761 Hamburg, Germany
[3]Helmholtz-Zentrum Dresden-Rossendorf, Bautzner Landstrasse 400, 01328 Dresden, Germany
[4]Institut für Theoretische Physik, Technische Universität Dresden, 01062 Dresden, Germany

TS, 0000-0001-7014-1069

Many phenomena described in relativistic quantum field theory are inaccessible to direct observations, but analogue processes studied under well-defined laboratory conditions can present an alternative perspective. Recently, we demonstrated an analogy of particle creation using an intrinsically robust motional mode of two trapped atomic ions. Here, we substantially extend our classical control techniques by implementing machine-learning strategies in our platform and, consequently, increase the accessible parameter regime. As a proof of methodology, we present experimental results of multiple quenches and parametric modulation of an unprotected motional mode of a single ion, demonstrating the increased level of real-time control. In combination with previous results, we enable future experiments that may yield entanglement generation using a process in analogy to Hawking radiation.

This article is part of a discussion meeting issue 'The next generation of analogue gravity experiments'.

THE ROYAL SOCIETY PUBLISHING

1. Introduction

Many intriguing processes suggested in the context of relativistic quantum field theory are currently inaccessible to direct observations, including, for example, particle creation in the early stages of our universe [1,2] and Hawking radiation [3]. Realizing similarly extreme conditions in a laboratory setting, to address, e.g., the Sauter–Schwinger effect [4], presents an outstanding task. However, establishing analogue processes can be an alternative approach to gain insight. This has been done using a variety of experimental platforms [5–13]. The trapped atomic ion platform is well suited to study fundamental quantum dynamical effects and ongoing developments in technology and methodology are propelled by the endeavour to work towards quantum computing applications and quantum metrology. Individual atomic ions feature unique fidelities in preparation, control and detection of quantum states and can preserve fragile quantum mechanical states for long durations due to their near ideal isolation from environments [14,15]. Recently, experiments demonstrated the creation of pairs of phonons, accompanied by the onset of spatial entanglement of two ions in a Coulomb coupled lattice [16]. Aspects of these results can be interpreted as an experimental analogue to an inflationary period of an early universe [17–19]. In our manuscript, we build on previous results and detail extensions of our toolbox, which are designed to play back extreme (non-adiabatic) conditions acting on carefully initialized quantum harmonic oscillators states. Using machine learning strategies, we substantially increase the level of our classical control techniques, implement fine tuned quenches and parametric modulations of the trapping potential to push the accessible parameter range further into the extreme. Finally, we outline steps for future realizations of a process that generates entanglement and present features that are analogue effects of Hawking radiation.

2. Methods

Our experimental set-up integrates a linear radio-frequency (rf) ion trap in an ultra-high vacuum chamber with a residual gas pressure below 10^{-8} Pa, and most of the relevant techniques employed here are described in detail in [16] and in an introductory review of the trapped-ion platform [14]. Here, we choose a single $^{25}Mg^{+}$ ion to implement a pseudo spin system (internal/electronic degree of freedom) on two suitable $S_{1/2}$ hyperfine ground states, labelled $|\downarrow\rangle$ and $|\uparrow\rangle$ and we employ Doppler cooling and subsequent resolved sideband cooling via two-photon stimulated-Raman transitions [14]. Using a collection of predesigned pulse sequences, we routinely initialize all three (decoupled) normal modes of the single ion to near the three-dimensional ground state (vacuum) with low mean thermal occupation numbers $\langle n\rangle_{\mathrm{th}} \ll 1$. We employ established techniques to reconstruct population distributions of the motional states by individually mapping them to the spin states, and subsequent electron shelving to distinguish $|\downarrow\rangle$ (bright state) from $|\uparrow\rangle$ (dark state), cf. [14]. The mapping technique is based on the coherent coupling of the internal and external degrees of freedom via resonant transitions $|\uparrow, n\rangle \leftrightarrow |\downarrow, n+1\rangle$ (blue sideband) and $|\downarrow, n\rangle \leftrightarrow |\uparrow, n-1\rangle$ (red sideband), where $|n\rangle$ denotes the corresponding number state of the individually addressed mode. In particular, we can determine amplitudes of the individual Fock states spanning thermal $\langle n\rangle_{\mathrm{th}}$, coherently displaced $\langle n\rangle_{\mathrm{dsp}}$ and squeezed $\langle n\rangle_{\mathrm{sq}}$ mode excitations. Radial confinement within the x–y-plane is dominated by an rf potential formed by a pair of electrodes connected to a single source and additional electrodes are referenced to rf ground. For our experiments, we require fast and precise control of the applied rf voltage U tuneable between 0 V and 800 V and oscillating at $\Omega_{\mathrm{rf}}/(2\pi) \simeq 56$ MHz. Our generator hardware system consists of a signal generator with fixed amplitude and frequency, a rf mixer controlled via an arbitrary waveform generator [20] delivering an output amplitude U_{c}, a high power amplifier (output power ≈ 40 dBm), a circulator and a helical resonator with a loaded quality factor $Q \approx 100$. The gold covered copper rf resonator is an integral part of our vacuum feedthrough and connects directly to both rf electrodes that present a capacitive load. We collect a signal from a dedicated pickup electrode that is capacitively coupled to the rf electrodes inside the vacuum chamber and monitor its amplitude $U_p \propto U$. In addition, we use six control electrodes, each controlled

by a channel of the arbitrary waveform generator, to fine tune ion positions, motional mode frequencies and orientations. Our real-time data acquisition system with timing resolution of 10 ns plays predefined waveforms $U_c(t)$ and controls laser pulse sequences on demand.

For simplicity, we ensure in our experiments by an appropriate choice of mode orientations and frequencies that modulations of U predominantly lead to non-adiabatic dynamics on one radial mode with frequency ω, pointing primarily along the x direction, as illustrated in figure 1*a*. To pre-estimate the dynamics along this mode and benchmark our experimental results, we can approximate the effect on the rf potential by the second-order term of a quasi-static (pseudo) potential expansion [14]. Therefore, we can reduce a corresponding numerical study on the dynamics of a single harmonic oscillator with time-dependent eigenfrequency $\omega(t)$ in following form [21]:

$$\hat{H}(t) = \hbar\omega(t)\left(\hat{a}^\dagger\hat{a} + \frac{1}{2}\right) - \frac{i\hbar}{4}\frac{\mathrm{d}\ln(\omega(t))}{\mathrm{d}t}\left[\hat{a}^2 - \left(\hat{a}^\dagger\right)^2\right]. \tag{2.1}$$

Here, time-independent basis operators $\hat{a}^\dagger$ and $\hat{a}$ defined for the initial mode frequency $\omega_{\mathrm{ini}} = \omega(0) \simeq 2\pi\ 2.8\,\mathrm{MHz}$ are used and we assume an initial vacuum state (experimentally we find $\langle n\rangle_{\mathrm{ini}} < 0.1$). Note, we record $\omega(U_{\mathrm{p}})$ in independent calibration measurements [16] and adjust our numerical estimations by explicitly setting $\omega(t) = \omega(U_{\mathrm{p}}(t))$. As long as the dynamics is adiabatic, i.e. the external rate of change $\dot{\omega}/\omega$ is small compared to ω, the wave function Ψ, describing the mode, can continuously adapt and stays close to the instantaneous ground state for all times. However, if the variation leads to violations of the adiabaticity condition ($\dot{\omega} \ll \omega^2$), the wave function deviates from the ground state. In that case, Ψ turns into an excited, squeezed state, and remains excited even when the variations come to a hold again. In the following, we distinguish between two non-adiabatic (extreme) regimes where eigenfrequency changes are (i) quenched (by rapid and strong pulses) and (ii) parametrically resonant to $2\omega_{\mathrm{ini}}$, the latter also recently shown in [22]. In case of (i), we focus on Gaussian shapes of the quenches characterized by their width $\delta\tau$ and amplitude $\Delta\omega$. We depict an exemplary result of our numerical calculations in figure 1*b*,*c* to illustrate the dynamical evolution of Ψ for $\dot{\omega}/\omega^2 \simeq 5$ and visualize the squeezing effect by a snapshot of the corresponding Wigner function $W(x,p)$ after the quench. In the phase space diagram, we reference the width of the ground state wave function $x_{\mathrm{ini}} = \sqrt{\hbar/(2m\omega_{\mathrm{ini}})}$ of the oscillator with mass m. In the following, we set x_{ini} to one (unitless) and quantify the squeezing amplitude by the average phonon number $\langle n\rangle_{\mathrm{sq}} = \sinh(r)^2$ using $r = \frac{1}{2}\mathrm{arccosh}[(\Delta x)^2 + (\Delta p)^2]$. For this, we define (dimensionless) position $\hat{x} = \hat{a}^\dagger + \hat{a}$ and momentum $\hat{p} = i(\hat{a}^\dagger - \hat{a})$ operators, corresponding expectation values $x(t) = \langle\hat{x}\rangle$ and $p(t) = \langle\hat{p}\rangle$, and variances $(\Delta x)^2(t) = \langle\hat{x}^2\rangle - \langle\hat{x}\rangle^2$ and $(\Delta p)^2(t) = \langle\hat{p}^2\rangle - \langle\hat{p}\rangle^2$. The final amount of squeezing critically depends on the details of the temporal evolution of $\omega(t)$ and we can iteratively adjust the parameters $\delta\tau$ and $\Delta\omega$ to find maximal $|r|$. In case of (ii), tunings of control parameters are less critical and sinusoidal modulation with amplitude $\delta\omega_{\mathrm{mod}}$, frequency $\omega_{\mathrm{mod}} = 2\,\omega_{\mathrm{ini}}$ and duration T_{mod} yield parametric amplification of vacuum fluctuations. Here, squeezing r scales linearly with $\Delta\omega_{\mathrm{mod}}$ and duration T_{mod}.

In particular, when implementing waveforms for quench squeezing in our experiments we need to be able to reproduce parameter settings with high accuracy. The finite bandwidth, significantly limited by the helical resonator, and specific characteristics, i.e. nonlinearities of the rf mixer and other components, of our current rf generator set-up lead to a non-trivial transfer function T. Consequently, input waveforms $U_c(t)$ are significantly distorted and our set-up produces outputs $U(t) = T(U_c(t))$ with maximal slew rates $\simeq 0.1\,\mathrm{kV}\,\mu\mathrm{s}^{-1}$. Consequently, we must pre-compensate for the transfer effects of the set-up, cp. [20]. We implement a machine-learning algorithm using the PyTorch package [23] that trains and optimizes input waveforms $U_c(t)$ by self-evaluating recorded $U_{\mathrm{p}}(t)$ to produce desired outputs $U(t)$ [24]. In this way, we are able to increase output slew rates by more than a factor of 10 to $\geq 1\,\mathrm{kV}\,\mu\mathrm{s}^{-1}$ and produce quench pulses U following the desired Gaussian shapes.

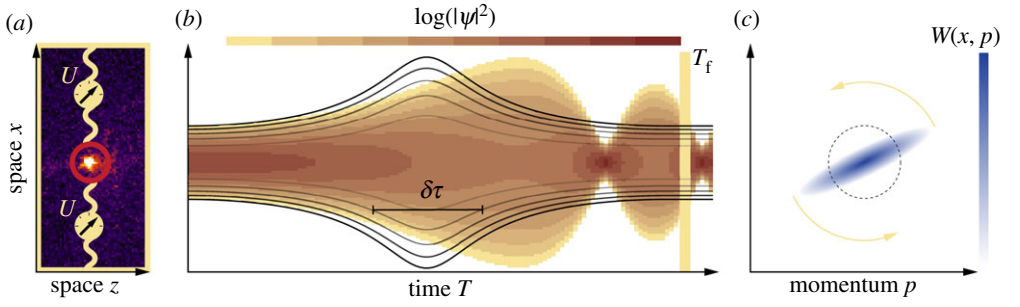

Figure 1. Single trapped-ion system for deterministic control of quantum harmonic oscillators under extreme conditions. (*a*) Image of the fluorescence light of a single trapped Mg^+ ion, superimposed with illustrations of the tunability of the ion's trapping potential (yellow wiggles with dials) using the control parameter U. In particular, by real-time tuning of U, we implement a time dependence of one of the normal mode frequencies $\omega(U(t))$. (*b*) A numerical simulation of the experimentally accessible parameter regime, where the trapping potential is strongly and rapidly switched (quenched), $\omega(t)$ is described by a Gaussian waveform with a characteristic duration width of $\delta\tau \simeq 0.5 \times 2\pi/\omega(0)$; black curves show corresponding equipotential lines. The dynamical evolution of the ground-state wave function is illustrated in colour code. (*c*) The Wigner function of the final state at T_f illustrates the phase space representation of a pure squeezed state with average phonon number $\langle n\rangle_{sq} \simeq 1$. Dashed circle indicates the extend of the ground state wave function. (Online version in colour.)

3. Results

In a first series of experiments, we implement sequences with a single quench of the rf potential (figure 2*a*) with ΔU^2 between zero and 5.4 dB and fixed $\delta\tau \simeq 0.18\,\mu$s to fine tune ion positions. In this parameter regime, we expect squeezing amplitudes of $\langle n\rangle_{sq} \leq 0.2$, supported by our numerical estimations. Residual ion displacements from the rf minimum translate to coherent displacement excitations by the quench [16]. Note, coherent displacement amplitudes are given by $\langle n\rangle_{dsp} = |\alpha|^2$ with $|\alpha(t)| = \sqrt{x^2(t) + p^2(t)}$. We probe spurious $\langle n\rangle_{dsp}$ as a function of the ion position in all three spatial directions, iteratively for increasing pulse amplitude. For optimized position parameter settings, we record $\langle n\rangle_{dsp,1}$ as a function of ΔU^2 and show resulting data points (black points) in figure 2*b*. Spurious displacements are significantly larger than the expected squeezing amplitudes. However, these parasitic excitations can be partially eliminated by coherent kicks back to the ground state via a second quench (purifying echo pulse). In this amplitude regime, this requires approximately the same amplitude after an optimized delay $\Delta\tau$; this second kick needs to be aimed towards the origin in phase space. Waiting durations $\Delta\tau$ between both pulses require tunings with an accuracy close to the time resolution of our data acquisition system and lead to a technical limitation of the purification effect. We quantify the purifying effect and plot reduced $\langle n\rangle_{dsp,2}$ as a function of ΔU^2 for two consecutive quenches (red data points) in figure 2*b*. A combined model fit to both data sets (single and double pulse sequences) yields a suppression by $\delta_p = \langle n\rangle_{dsp,1}/\langle n\rangle_{dsp,2} = 51(2)$. In figure 2(*c*, top), we illustrate this effect for maximal pulse amplitudes by plotting corresponding Wigner functions $W_1(x,p)$ and $W_2(x,p)$ for the single and double pulse sequence, respectively.

In a second series of experiments, we apply higher pulse amplitudes with ΔU^2 between 5.8 and 6.3 dB to produce significantly squeezed states via the two quench sequence. Ideally, the second pulse fulfils two purposes: (i) reducing spurious displacements (figure 2*c*), and (ii) amplifying squeezing seeded by the first quench. We iteratively adjust the amplitude of the second quench $U + \delta U$ and $\Delta\tau$ in sets of dedicated calibration sequences for achieving close to ideal conditions for all probed ΔU^2. Data within this amplitude regime are shown in the grey region of figure 2*b*. Here, we fit our results with contributions of squeezing $\langle n\rangle_{sq}$ (blue data points) and coherent displacements $\langle n\rangle_{dsp}$ (red data points), and find $\langle n\rangle_{sq} \simeq \langle n\rangle_{dsp}$ within the probed regime. We show the reconstructed phonon distribution for $\langle n\rangle_{sq} = 2.13(9)$ and $\langle n\rangle_{dsp} = 2.4(8)$ and corresponding

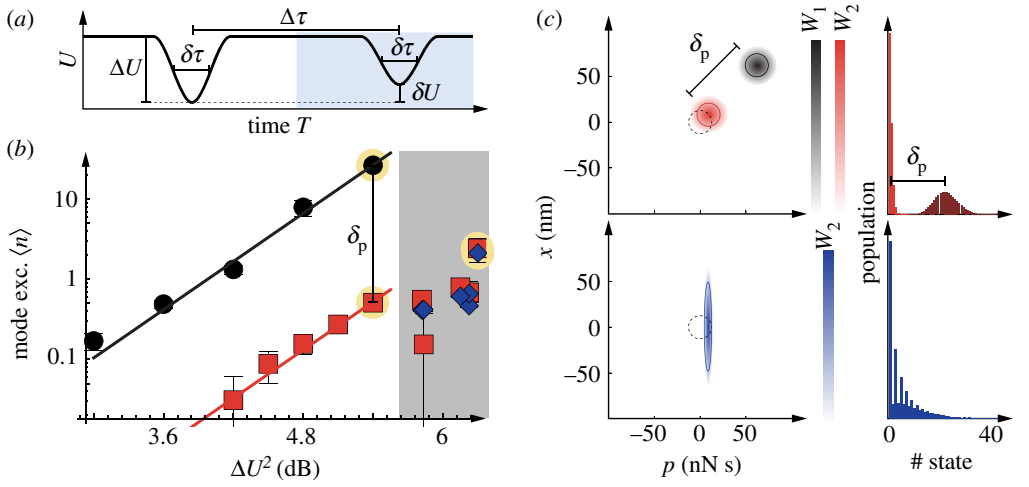

Figure 2. Quench squeezing applied to a single ground-state cooled ion. (*a*) Schematic of the pulse sequence with an optional purifying pulse to mitigate spurious displacements within the rapidly tuned trapping potential. The trapped ion is cooled initially near to the three-dimensional ground state of motion with $\langle n\rangle_{\mathrm{ini}} < 0.1$ for the corresponding mode. (*b*) A single quench with variable amplitude ΔU^2 up to 5 dB and fixed width $\delta\tau \simeq 0.18\,\mu$s yields significant parasitic coherent displacement $\langle n\rangle_{\mathrm{dsp}}$ (black points). The optional second quench with optimized waiting duration $\Delta\tau$ and amplitude $(\Delta U - \delta U)^2$ (with the same width $\delta\tau$) kicks displacements back to the origin (red squares), we find an effective suppression of 51(2). For even higher quench amplitudes (grey region) using optimized double-pulse sequences, we detect excited coherent states with comparable contributions of squeezing $\langle n\rangle_{\mathrm{sq}}$ (blue diamonds) and residual displacements $\langle n\rangle_{\mathrm{dsp}}$ (red squares). (*c*) Phase space illustrations of the Wigner functions and detected Fock state distributions for exemplary final states after a single and double pulse sequence with $\Delta U^2 \simeq 5$ dB (top) and higher amplitude $\Delta U^2 \simeq 6.3$ dB (bottom) resulting in a squeezing of $r = 1.1(3)$. (Online version in colour.)

Wigner function, produced by sequences with $\Delta U^2 = 6.3\,\mathrm{dB}$ and $\delta U^2 = 0.27(3)\,\mathrm{dB}$ in figure 2(*c*, bottom). Note, the quench amplitude of the second pulse needs to be lowered with respect to the first pulse as the seeded displaced and squeezed states are more sensitive to forces than the initial vacuum state [16], since operators for squeezing and coherent displacement do not commute.

In a final series of experiments, we benchmark parametric amplification sequences for generation of squeezed states that are intrinsically robust against parasitic displacements (figure 3*a*). In preparation of these experiments, we calibrate ω_{mod} while applying the amplification sequence for fixed $\delta\omega_{\mathrm{mod}} \simeq 2\pi\,8\,\mathrm{kHz}$ and $T_{\mathrm{mod}} \simeq 196 \times 2\pi/\omega_{\mathrm{mod}}$. We find $\omega_{\mathrm{mod}} = 1.979(1)\,\omega$ and attribute this detuning to an effective, negative offset of average U during the amplification sequence resulting predominantly from non-linearities in our rf generator set-up. In figure 3*b*, we show reconstructed squeezed state amplitudes $\langle n\rangle_{\mathrm{sq}}$ as a function of T_{mod} and a corresponding model fit to the data using: $\sinh(2\pi\, g\, T_{\mathrm{mod}})^2$. Here, g denotes the parametric coupling strength [22] and we determine a best fit value of $g/(2\pi) = 4.64(6)\,\mathrm{kHz}$. All data are consistent with $\langle n\rangle_{\mathrm{dsp}} = 0$, indicating that close to pure squeezed states are produced, see inset of figure 3*b* that shows the Wigner function for maximal T_{mod}.

A next-generation experiment builds on our current findings in combination with previous results that benefit from intrinsic features of a two-ion crystal [16,19] and enable studies of entanglement properties. Similar to the case of cosmic inflation [16,19], we can identify analogies of our envisioned experiment to delicate features of Hawking radiation expected to appear in vicinity of black holes, i.e. resulting during black-hole evaporation. In particular, we can access an effective Hawking temperature T_{H} regime by tuning our quench and/or modulation parameters [16]. Adjusting the time-dependence of the mode frequency mimics the tearing apart of quantum vacuum fluctuations near the black hole horizon by the strong gravitational field.

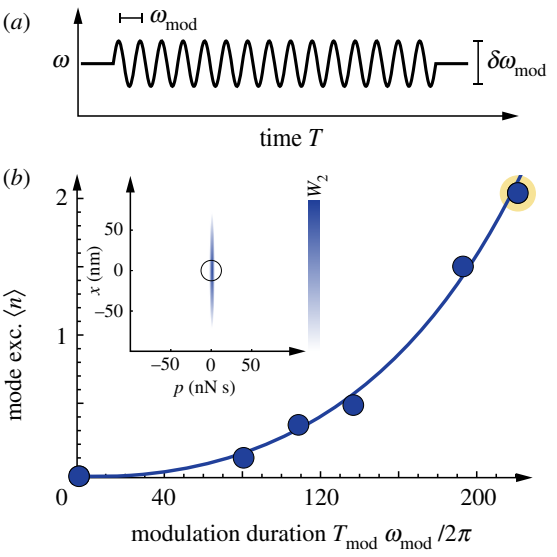

Figure 3. Intrinsically robust, parametric modulation sequence for pure squeezing. (*a*) Illustration of a parametric modulation of the trapping potential U. We modulate with fixed frequency $\omega_{\mathrm{mod}} \simeq 2\omega$ and amplitude $\delta\omega_{\mathrm{mod}} \simeq 2\pi$ 8 kHz for a variable duration T_{mod}. (*b*) Experimental results for the motional excitation as a function of T_{mod}; the data are consistent with $\langle n \rangle_{\mathrm{dsp}} \equiv 0$. (Inset) Wigner function of the detected final state for $T_{\mathrm{mod}} \simeq 224 \times 2\pi/\omega_{\mathrm{mod}}$ illustrating a squeezing of $r = 1.16(5)$. (Online version in colour.)

To discuss extended experimental sequences that can study such effects, we outline a three step process that deterministically (i) seeds, (ii) generates, and (iii) transfers entanglement of the spatial degrees of freedom of two ions into their electronic degrees of freedom, enabling the direct quantification of the amount of entanglement. In figure 4, we illustrate ions A and B that are initialized close to the ground states in all motional degrees of freedom. Ions align along the direction of the weakest confinement, here, the z axis of the trap, interact individually with the common trapping potential and with each other due to their mutual Coulomb interaction. In this scenario, the initiation step (i) will produce a squeezed state of a common radial mode, for example via modulation of the axial trapping potential assisted by the Coulomb interaction [19], or (directly) via modulation of the radial trapping potential [16]. During step (ii), the strongly coupled ion pair will effectively become uncoupled using state-of-the-art separation techniques [25]. This step needs to be carefully calibrated to avoid further excitation of the squeezed degrees of freedom to yield a distant (non-local) entangled pair of ions. Finally, step (iii), coherently couples the individual (entangled) oscillator states to the ions' electronic degrees of freedom. The subsequent read out of the electronic states enables reconstruction of the individual phonon distributions. These phonon distributions can be described by an expected mixed-state distribution, parametrized by T_{H}. Note, for maximal transfer to the electronic states, the entanglement is robustly stored and can be quantified directly.

4. Conclusion

Squeezing is one of the major differences between classical and quantum physics and underlies many intriguing phenomena, ranging from parametric down-conversion in quantum optics to cosmological particle creation and Hawking radiation. Naturally, as an inherently non-classical property, the controlled creation and detection of squeezed states in the laboratory can be a challenging task. A frequently used option is parametric resonance. In a simplified harmonic oscillator picture, this mechanism can be visualized by small oscillations of the oscillator potential

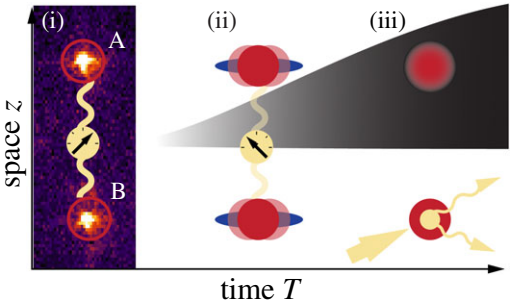

Figure 4. Next-generation experiments in analogy to Hawking radiation building on our demonstrated toolbox. Similar to our recent results [16], two co-trapped ions, labelled A and B, are used in this scenario to implement an extended experimental sequence that follows three crucial steps. (i) Trapping parameters are adjusted to yield strong coupling (wiggle with dial on high, i.e. strong axial confinement) between the two ions and tailored waveform sequences are played back to squeeze a common mode of motion. (ii) After this significant amplification of the quantum vacuum fluctuations, the inter-ion coupling is adiabatically reduced (wiggle with dial on low, i.e. reduced axial confinement) to yield two effectively disconnected ions in a spatially entangled state. (iii) The uncoupled (ions are located in individual wells) motional state of ion B is read out using an appropriate laser pulse sequence, projecting also the distant (non-local) ion A into a well-defined state. On average of multiple repetitions of such sequence, the detected phonon distribution is expected to appear as a mixed state distribution, parametrized by an effective Hawking temperature T_H. Further, a Bell test can be performed in our platform and requires additional local measurements on ion A. The fidelity of the full final state can be used to check for spurious systematic effects that are introduced during such sequence. (Online version in colour.)

at twice the frequency of the oscillator. A sufficiently large number of these small oscillations can then generate a measurable amount of squeezing, which is the fundamental mechanism behind parametric down-conversion, for example. An alternative mechanism for generating squeezing is a large and rapid (i.e. non-adiabatic) change of the oscillator potential. This process is more analogous to cosmological particle creation and Hawking radiation, where the quantum vacuum fluctuations are torn apart by the extreme external conditions—which correspond to large variations of the oscillator potential. Realizing such a process in the laboratory, however, is even more challenging. Here, we report on the generation of squeezed states in the motional degrees of freedom in ion traps. For a single ion, we achieve a squeezing strength of $r = 1.1(3)$ via the timed two-pulse sequence depicted in figure 2*a*. This sequence is advantageous because of two main reasons. First, the initial preparation and the final read-out are done best at strong radial confinement, i.e. large oscillator frequency. Second, the destructive interference of coherent displacements via the two pulses facilitates a strong reduction of the unwanted background, similar to state-of-the-art approaches for dynamical suppression of noise fields and for arbitrary quantum control via filter transfer functions (e.g. [26,27] and references within). Since the mapping from the input voltage (as a function of time) to the output voltage (generating the trap potential) is nonlinear as well as non-local in time, generating the two-pulse sequence depicted in figure 2*a* is a non-trivial task. Via a machine learning algorithm, we optimized the input signal in order to achieve an output as close as possible to the desired sequence. For comparison, we also modelled the process of parametric resonance (figure 3). In contrast to Hawking radiation (corresponding to a ramp of the potential), this process is more analogous to scenarios for the process of re-heating at the end of the inflationary epoch in the early Universe (or to parametric down-conversion in quantum optics), see also [22]. For two ions, a timed two-pulse sequence, as depicted in figure 2*a*, yields a squeezed state of the motional out-of-phase mode. As an additional feature of this set-up, entanglement between the two ions is generated in their motional states and could, in principle, be transferred to their electronic states. Owing to this entanglement, the two-ion case is a closer analogue to Hawking radiation or cosmological particle creation. In this analogy, one ion represents the Hawking radiation emitted by the black hole, while the other ion corresponds to its partner falling into the black hole. Owing to the entanglement between

the two ions, their pure quantum state appears as a mixed state (like a thermal ensemble) when only one ion is considered. The entanglement between the two ions caused by the non-adiabatic ramping manifests itself in a non-zero entropy of the mixed state of one ion—analogous to the entanglement entropy of Hawking radiation, which is often discussed in relation to the Beckenstein–Hawking entropy of black holes. As an outlook, one might squeeze two or more ions via parametric resonance (in analogy to the re-heating scenario mentioned above) as in figure 3 and compare the results to the non-adiabatic ramps considered here. The next step could be to consider more general time dependencies which opens the door for more analogies (e.g. the Sauter–Schwinger effect). As another generalization, one could take into account more modes (not just the out-of-phase mode), which would facilitate the study of frequency-dependent spectra. Even though it is non-trivial to achieve full quantum control of a larger number of ions, many laboratories worldwide are pursuing this goal—mostly motivated by large-scale quantum information processing applications.

Data accessibility. Raw data were provided as electronic supplementary material.

Authors' contributions. M.W., J.P.S. and U.W. participated in the design of the experiment, built the experimental apparatus, collected data and analysed the results. C.F. and R.S. detailed the theoretical aspects of the analogy. F.H., P.K., C.F., R.S. and T.S. participated in design and analysis of the experiment. All authors discussed the results and the text of the manuscript.

Competing interests. The author(s) declare that they have no competing interests.

Funding. This work was supported by the Deutsche Forschungsgemeinschaft (DFG) (grant nos. 237456450 (SCHA 973/6-2) and 278162697 (SFB 1242)] and the Georg H. Endress foundation.

References

1. Schrödinger E. 1939 The proper vibrations of the expanding universe. *Physica* **6**, 899–912. (doi:10.1016/S0031-8914(39)90091-1)
2. Parker L. 1969 Quantized fields and particle creation in expanding universes. I. *Phys. Rev.* **183**, 1057–1068. (doi:10.1103/PhysRev.183.1057)
3. Hawking SW. 1974 Black hole explosions? *Nature* **248**, 30–31. (doi:10.1038/248030a0)
4. Sauter F. 1931 Über das Verhalten eines Elektrons im homogenen elektrischen Feld nach der relativistischen Theorie Diracs. *Zeitschrift für Physik* **69**, 742–764. (doi:10.1007/BF01339461)
5. Belgiorno F, Cacciatori SL, Clerici M, Gorini V, Ortenzi G, Rizzi L, Rubino E, Sala VG, Faccio D. 2010 Hawking radiation from ultrashort laser pulse filaments. *Phys. Rev. Lett.* **105**, 203901. (doi:10.1103/PhysRevLett.105.203901)
6. Lahav O, Itah A, Blumkin A, Gordon C, Rinott S, Zayats A, Steinhauer J. 2010 Realization of a sonic black hole analog in a Bose–Einstein condensate. *Phys. Rev. Lett.* **105**, 240401. (doi:10.1103/PhysRevLett.105.240401)
7. Wilson CM, Johansson G, Pourkabirian A, Simoen M, Johansson JR, Duty T, Nori F, Delsing P. 2011 Observation of the dynamical Casimir effect in a superconducting circuit. *Nature* **479**, 376–379. (doi:10.1038/nature10561)
8. Weinfurtner S, Tedford EW, Penrice MCJ, Unruh WG, Lawrence GA. 2011 Measurement of stimulated Hawking emission in an analogue system. *Phys. Rev. Lett.* **106**, 021302. (doi:10.1103/PhysRevLett.106.021302)
9. Jaskula JC, Partridge GB, Bonneau M, Lopes R, Ruaudel J, Boiron D, Westbrook CI. 2012 Acoustic analog to the dynamical Casimir effect in a Bose-Einstein condensate. *Phys. Rev. Lett.* **109**, 220401. (doi:10.1103/PhysRevLett.109.220401)
10. Lähteenmäki P, Paraoanu GS, Hassel J, Hakonen PJ. 2013 Dynamical Casimir effect in a Josephson metamaterial. *Proc. Natl Acad. Sci. USA* **110**, 4234–4238. (doi:10.1073/pnas.1212705110)
11. Steinhauer J. 2016 Observation of quantum Hawking radiation and its entanglement in an analogue black hole. *Nat. Phys.* **12**, 959–965. (doi:10.1038/nphys3863)
12. Euvé LP, Michel F, Parentani R, Philbin TG, Rousseaux G. 2016 Observation of noise correlated by the hawking effect in a water tank. *Phys. Rev. Lett.* **117**, 121301. (doi:10.1103/PhysRevLett.117.121301)

13. Eckel S, Kumar A, Jacobson T, Spielman IB, Campbell GK. 2018 A rapidly expanding Bose–Einstein condensate: an expanding universe in the lab. *Phys. Rev. X* **8**, 021021. (doi:10.1103/physrevx.8.021021)
14. Leibfried D, Blatt R, Monroe C, Wineland DJ. 2003 Quantum dynamics of single trapped ions. *Rev. Modern Phys.* **75**, 281–324. (doi:10.1103/RevModPhys.75.281)
15. Wineland DJ. 2013 Nobel lecture: superposition, entanglement, and raising Schrödinger's cat. *Rev. Mod. Phys.* **85**, 1103–1114. (doi:10.1103/RevModPhys.85.1103)
16. Wittemer M, Hakelberg F, Kiefer P, Schröder J-P, Fey C, Schützhold R, Warring U, Schaetz T. 2019 Phonon pair creation by inflating quantum fluctuations in an ion trap. *Phys. Rev. Lett.* **123**, 180502. (doi:10.1103/PhysRevLett.123.180502)
17. Alsing PM, Dowling JP, Milburn GJ. 2005 Ion trap simulations of quantum fields in an expanding universe. *Phys. Rev. Lett.* **94**, 220401. (doi:10.1103/PhysRevLett.94.220401)
18. Schützhold R, Uhlmann M, Petersen L, Schmitz H, Friedenauer A, Schätz T. 2007 Analogue of cosmological particle creation in an ion trap. *Phys. Rev. Lett.* **99**, 201301. (doi:10.1103/PhysRevLett.99.201301)
19. Fey C, Schaetz T, Schützhold R. 2018 Ion-trap analog of particle creation in cosmology. *Phys. Rev. A* **98**, 33407. (doi:10.1103/PhysRevA.98.033407)
20. Bowler R, Warring U, Britton JW, Sawyer BC, Amini J. 2013 Arbitrary waveform generator for quantum information processing with trapped ions. *Rev. Sci. Instrum.* **84**, 033108. (doi:10.1063/1.4795552)
21. Silveri MP, Tuorila JA, Thuneberg EV, Paraoanu GS. 2015 Quantum systems under frequency modulation. *Rep. Prog. Phys.* **80**, 056002. (doi:10.1088/1361-6633/aa5170)
22. Burd SC, Srinivas R, Bollinger JJ, Wilson AC, Wineland DJ, Leibfried D, Slichter DH, Allcock DTC. 2019 Quantum amplification of mechanical oscillator motion. *Science* **364**, 1163–1165. (doi:10.1126/science.aaw2884)
23. *An open source machine learning framework*. https://pytorch.org.
24. Schroeder JP. *et al*. In preparation. Improve classical control of trapped ions via machine-learning techniques.
25. Jost JD, Home JP, Amini JM, Hanneke D, Ozeri R, Langer C, Bollinger JJ, Leibfried D, Wineland DJ. 2009 Entangled mechanical oscillators. *Nature* **459**, 683–685. (doi:10.1038/nature08006)
26. Biercuk MJ, Uys H, VanDevender AP, Shiga N, Itano WM, Bollinger JJ. 2009 Optimized dynamical decoupling in a model quantum memory. *Nature* **458**, 996–1000. (doi:10.1038/nature07951)
27. Soare A, Ball H, Hayes D, Sastrawan J, Jarratt MC, Mcloughlin JJ, Zhen X, Green TJ, Biercuk MJ. 2014 Experimental noise filtering by quantum control. *Nat. Phys.* **10**, 825–829. (doi:10.1038/nphys3115)